Hindawi
Journal of Nanomaterials
Volume 2020, Article ID 4370172, 9 pages
https://doi.org/10.1155/2020/4370172

Research Article

Optimization of Milling Procedures for Synthesizing Nano-$CaCO_3$ from *Achatina fulica* Shell through Mechanochemical Techniques

O. J. Gbadeyan,[1] **S. Adali**,[1] **G. Bright**,[1] **B. Sithole**,[2] **and S. Onwubu**[3,4]

[1]*School of Engineering, Discipline of Mechanical Engineering, University of Kwazulu-Natal, South Africa*
[2]*School of Engineering, Discipline of Chemical Engineering, University of Kwazulu-Natal, South Africa*
[3]*Biorefinery Industry Development Facility, Council for Scientific and Industrial Research, South Africa*
[4]*Dental Sciences Department, Durban University of Technology (DUT), Durban, South Africa*

Correspondence should be addressed to O. J. Gbadeyan; toyin2good@gmail.com

Received 14 March 2020; Revised 9 May 2020; Accepted 13 May 2020; Published 4 July 2020

Academic Editor: Bhanu P. Singh

The possibility of obtaining calcium carbonate nanoparticles from *Achatina fulica* shell through mechanochemical synthesis to be used as a modifying filler for polymer materials has been studied. The process of obtaining calcium carbonate nanopowders includes two stages: dry and wet milling processes. At the first stage, the collected shell was dry milled and undergone mechanical sieving to ≤50 μm. The shell particles were wet milled afterward with four different solvents (water, methanol, ethylene glycol, and ethanol) and washed using the decantation method. The particle size and shape were investigated on transmission electron microscopy, and twenty-three particle counts were examined using an iTEM image analyzer. Significantly, nanoparticle sizes ranging from 11.56 to 180.06 nm of calcium carbonate was achieved after the dry and wet milling processes. The size particles collected vary with the different solvents used, and calcium carbonate synthesis with ethanol offered the smallest organic particle size with the average size ranging within 13.48-42.90 nm. The effect of the solvent on the chemical characteristics such as the functional group, elemental composition, and carbonate ion of calcium carbonate nanopowders obtained from *Achatina fulica* shell was investigated. The chemical characterization was analyzed using Fourier transform infrared (FTIR) and a scanning electron microscope (SEM) equipped with an energy-dispersive spectroscope (EDX). The effect of milling procedures on the mechanical properties such as tensile strength, stiffness, and hardness of prepared nanocomposites was also determined. This technique has shown that calcium carbonate nanoparticles can be produced at low cost, with low agglomeration, uniformity of crystal morphology, and structure from *Achatina fulica* shell. It also proved that the solvents used for milling have no adverse effect on the chemical properties of the nano-$CaCO_3$ produced. The loading of calcium carbonate nanoparticles, wet milled with different solvents, exhibited different mechanical properties, and nanocomposites filled with methanol-milled nano-$CaCO_3$ offered superior mechanical properties.

1. Introduction

Nanosized calcium carbonate ($CaCO_3$) has received noteworthy consideration for several applications due to its availability, advantageous mechanical strength, and thermal stability [1]. It is commonly used as filler or reinforcement for polymeric materials, papers, and paints. This carbon-based material is obtained from several resources such as rock, humans, and animal waste through different methods. Over many decades, montmorillonite and kaolinite with a high concentration of $CaCO_3$ commonly referred to as nanoclay are commonly used and soured from rock and synthesized using either gas pressure blasting or explosion method [2–4]. Studies conducted confirmed the effectiveness of nanoclay in improving several composite properties [5, 6]. However, it has been discovered that the end-of-life of the

composite produced with nanoclays tends to have negative impacts on human health, and, at times, the composite is more expensive when compared to naturally sourced fillers [7]. These drawbacks consequently have reduced the use of this filler in some countries.

The harmful impact of the abovementioned fillers and factors such as climate change compelled materials scientist to source for alternative filler material. The fillers are sourced from natural resources that not only offer suitable filler material properties but also meet societal needs and support global sustainability. Consequently, in recent decades, calcium carbonate ($CaCO_3$) of different particle sizes extracted from natural resources such as bones, horns, and animal shells is used as reinforcement to enhance thermal stability, degradation, strength, and physical properties of polymeric materials [8].

Several types of research have investigated the functional group, elemental composition, and minerals present in eggshell, mollusk shell, and animal bone [8–11]. These natural resources were discovered to have a higher content of calcium carbonate ($CaCO_3$), especially eggshell, which was confirmed to have about 95% of $CaCO_3$ [12–14]. Furthermore, mollusk shell, oyster shell, and animal bone have been investigated for $CaCO_3$, and they were found to have adequate filler-appropriate properties for different applications. Consequently, calcium carbonate produced from animal waste has been suggested to be used as an alternative to commercial $CaCO_3$ for some applications, which include but not limited to the dental and medical applications [8, 9, 15–18]. The mechanism behind the physical properties of shell structure has been studied [19, 20]. Filetin et al. [19] investigated microhardness of *Pinna pectinata* (Pinnidae), with the Adriatic Sea mollusk shell structure as a function of the indentation load. The result proved that the microhardness of the shell depends on the load for the nacreous (inner layer of the shell) and prismatic (outer layer of the shell) structures. Furthermore, the microhardness value measure for the outer layer was higher than that for the inner layer with a lesser margin. Besides, a notable aragonite platelet structure was seen in between the nacreous and prismatic predominant normal stress, preventing interlamellar sliding/plastic deformation of the shell. This study was consistent with our previous investigation on the physical and morphological study of *Achatina fulica* shell. The layer of aragonite was referred to as reinforcement and served as the main functional mechanism that prevents plastic deformation which resulted in high resistance to indentation, resulting in relatively high microhardness and tensile strength properties [20]. However, there is limited literature about $CaCO_3$, synthesized from these natural resources, being used either as a filler material to fabricate composite or as polymer material reinforcement. This output may be because milling a large quantity of these materials to smaller particle sizes comes with many challenges, which include but not limited to particle agglomeration.

Despite the availability of numerous milling techniques used for small organic particle synthesis, the mechanochemical technique has been found to be most effective [4, 21]. This organic synthesis mechanism has been regarded as a significant change towards achieving the sustainable and efficient process of producing small molecular sizes of grains [22]. Numerous researchers confirmed that mechanochemical techniques are a branch of chemistry that covers any chemical transformations induced mechanically or physiochemical changes of the material of any state of combination due to the influence of mechanical energy such as friction, compression, or shear [15, 23–26]. A mechanochemical procedure such as hand grinding or ball milling has been reported to influence the structure and composition of materials. Consequently, it brings about an opportunity for the preparation and fabrication of nanomaterial particles using top-down tactics [27].

Ball mill is a high-energy mill process especially used for an energy-intensive process like mechanical alloying, mechanochemistry, or mechanical activation. Planetary ball mill is used to determine the dependence of process efficiency using milling parameters such as ball size and number, mill geometry, and velocity of the rotating parts. However, the maximum efficiency of the grinding process achieved with high-density balls, and higher rotation speed seems to provide materials with higher impact energy in comparison with small, low-density balls and lower rotation speed [28, 29].

The planetary ball mill theory and its efficient procedure for producing small molecular sizes of grains achieved using the mechanochemical technique made it a promising candidate for solvent-free synthesis [21, 30, 31]. However, solvent-free synthesis may not apply to all materials, especially calcium carbonate-based materials, where the agglomeration of particles is dominant. Research studies have proved that dry milling technique causes a large agglomeration of the particles during synthesis. Most times, this results in a bimodal size distribution, which weakens the bond in nanocomposites [32–35]. Having this in mind, this present study deals with the optimization of milling procedures for synthesizing nano-$CaCO_3$ from *Achatina fulica* shell through mechanochemical (wet milling) techniques using different solvents. It further investigates the consequence of the solvent on the reinforcement effect of the nano-$CaCO_3$ on polymeric material.

2. Experimental Details

2.1. Raw Material Collection, Preparation, and Synthesis. Epoxy resin and hardener supplied with the trade name of LR 30 and LH 30 (medium) was used as a binder.

Achatina fulica snail shells collected from the University of Kwazulu-Natal, Westville campus soccer pitch, were washed and disinfected. Snail shells were soaked in a solution of water and 5% diluted household sodium hypochlorite for seven hours. Afterward, they were rinsed with distilled water and dried in the oven at 150°C for 20 mins to ensure absolute dehydration.

2.1.1. Nano-$CaCO_3$ Synthesis. The clean shells were kept under room temperature for 24 hours to dry before milling. The milling process was done in two stages. The first stage was dry milling, and the second was wet milling. At the first stage, 30 g of dried *Achatina fulica* snail shells was measured and dry milled in a planetary ball mill (Retsch® PM 100) to obtain fine particles [12, 36]. The milling setup comprises

50 stainless steel balls of 10 mm diameter and a 500 mL stainless steel jar (inner diameter of 100 mm). The snail shells were milled at 450 rpm for 30 minutes in a clockwise direction. The shell powder after the milling process was sieved using a mechanical sieving shaker (Retsch, AS 200 basics, Germany) to a particle size of ≤50 μm. In the second stage, the collected snail shell powder was wet milled to achieve nanoparticles. Accordingly, 30 g of snail shell particle size of ≤50 μm was measured into the 500 mL stainless steel jar. After that, 100 mL of a different solvent such as water, methanol, ethylene glycol, and ethanol was added differently and wet milled at 450 rpm for 258 mins in a clockwise direction. Subsequently, mixtures of fine particles and solvent were separated by removing the liquid layer that is free of a precipitate using the decantation method. To ensure the total removal of the solvent, settled particles were washed by adding distilled water and separated using the decantation method. This process was repeated five times to ensure the cleanness of fine particles. Then, particles were dried in the oven at 35°C for 72 hours. The fine powders obtained after that were characterized to establish the successful synthesis of the $CaCO_3$.

2.2. Characterization Approaches

2.2.1. High-Resolution Electron Microscopy. The particle size, shape, and distribution of snail shell particles milled with different solvents were observed under a transmission electron microscope (TEM). The investigation was conducted on JEM Jeol 2100 (Japan). Before this investigation, a small amount of snail shell powder was dispersed in 10 mL of ethanol and sonicated at 10 kV for 10 mins. Afterward, a thin cross section of cryomicrotomed specimens was prepared using a Leica microtome and placed on carbon copper grids. The TEM image was further analyzed on iTEM analyzer software, version 5.0.1 (Japan), to determine the range of particle sizes.

2.2.2. Fourier Transform Infrared Spectroscopy. The Fourier transform infrared (FTIR) spectra were measured to identify the functional group constituents of snail shell particles milled with different solvents. A PerkinElmer Universal ATR spectrometer was used for investigation. A small quantity of each sample was placed in the sample pouch. Subsequently, an initial background check was conducted before scanning within the range of 550-4000 cm^{-1} at a resolution of 4 cm^{-1}.

2.2.3. Scanning Electron Microscope. The chemical composition of the shell was determined on the Zeiss Ultra FEG-SEM field emission scanning electron microscope (SEM) equipped with an energy-dispersive spectroscope (EDX). Before SEM (field emission, Carl Zeiss) observation, the surface was coated with a thin, electric conductive gold film to prevent a buildup of electrostatic charge.

2.2.4. Nanocomposite Preparation. Nanocomposites were prepared using the conventional resin casting method. To facilitate shell particle dispersion and to reduce matrix viscosity, 100 wt.% of epoxy resin was measured into the beaker using a Snowrex digital electronic scale with 0.1 g and heated up to 70°C. Subsequently, 2 wt.% of $CaCO_3$ nanoparticles from shell particles was slowly incorporated into the matrix and mixed using a mechanical stirrer at 500 rpm for one hour to ensure homogeneous dispersion of shell particles. Nanocomposites were taken off the stirrer and were allowed to cool down to room temperature. Then, the catalyst was added to nanocomposites at a mixing ratio of 100-30 wt.%. The blend was thereafter poured into an open mold to have a composite panel and allowed to cure for two days. To facilitate the easy removal of the nanocomposite panel, the wax was applied to the inner surface of the plastic mold before pouring. The mechanical strength of the fabricated nanocomposite panel was investigated after 15 days.

2.3. Mechanical Testing. Mechanical tests such as tensile, hardness, and impact were performed on wholly cured composite panel samples obtained after fifteen days of casting.

2.3.1. Tensile. The tensile strength and stiffness of nanocomposite were determined according to the ASTM D3039 test standard. The test was carried out on samples using a Lloyd universal testing machine (Model 43) fitted with a 30 kN load cell. Five samples were tested at ambient temperature, and the constant crosshead speed of testing used was 1.3 mm/min. The mean value of the five samples was reported.

2.3.2. Hardness. The Barcol impressor hardness tester commonly used for composite material was used to determine the hardness property of composite panel samples. The test was performed according to the ASTM D2583 test standard. A standard impressor with a steel truncated cone (6.82 height and a tip diameter of 0.55 mm) was used at an angle of 26°. This intender was positioned on the surface of the composite panel, and a uniform downward press was applied by hand, and readings were collected directly from the dial indicator. Twenty-five indentation readings were randomly collected on the sample, and the mean values were used for graphical illustration and discussion.

3. Result and Discussion

3.1. Characterization. Figure 1 presents the FTIR spectra of the raw snail shell (*Achatina fulica*) powder and $CaCO_3$ nanoparticle obtained through ball milling mechanochemical techniques using different solvents. Numerous bands were seen within the range of 550 cm^{-1}-4000 cm^{-1}.

A relatively few FTIR spectra peaks, typically associated with the stretching vibration of the functional group, were observed.

Noticeably, the spectra for the raw shell and synthesized nano-$CaCO_3$ are quite different within the functional group region. On the contrary, insignificant different FTIR spectra peaks and bends were observed between nano-$CaCO_3$ wet milled and synthesized with different solvents such as ethylene glycol, ethanol, water, and methanol. Furthermore, the raw shell FTIR spectra display absorption peaks of calcite at about 713 cm^{-1} and 873 cm^{-1}, while nano-$CaCO_3$ synthesized with different solvents such as ethylene glycol, ethanol, water, and methanol shows the absorption peaks of aragonite at around 712 cm^{-1}, 854 cm^{-1}, and 1083 cm^{-1}. The peaks of

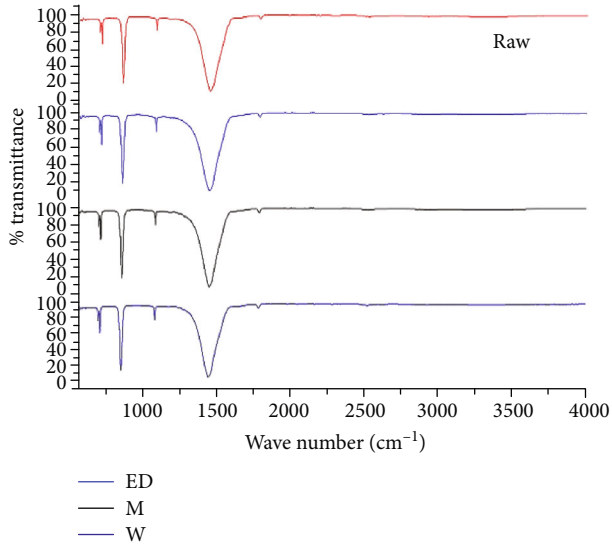

Figure 1: Fourier transform infrared (FTIR) spectra of the raw snail shell and snail shell milled with ethanol (E), ethylene glycol (ED), methanol (M), and water (W).

calcite displayed at 713 cm^{-1} and 873 cm^{-1} were accredited to the out-of-plane bending and in-of-plane bending vibration modes, asymmetric and symmetric stretching for calcium carbonate (CO_3^{2-}) molecules.

Furthermore, a very close prominent absorption peak is observed for both the raw shell powder and the synthesized $CaCO_3$ nanoparticle (1474 cm^{-1} and 1448 cm^{-1}) at the functional group region. These were associated with the presence of carbonate ions in both materials. The FTIR spectra observed for the raw shell powder were consistent with the literature for calcite [12, 16, 37, 38]. The absorption peaks of aragonite displayed at around 1083 cm^{-1} of $CaCO_3$ nanoparticles synthesized with different solvents such as ethylene glycol, ethanol, water, and methanol could be attributed to symmetric carbonate stretching vibration, and the absorption peaks of aragonite displayed at around 854 cm^{-1} were accredited to carbonate out-of-plane bending vibrations [37–39]. Additionally, the carbonyl group C=O bending identified around 1788 cm^{-1} was attributed to solvent (ethylene glycol, ethanol, water, and methanol) used for mechanochemical processes. Similarly, the tiny slope of carboxyl group O-H stretching is observed at around 2533 cm^{-1}. This is associated with traces of water molecules. This suggests that $CaCO_3$ nanoparticles can be obtained from snail shell *Achatina fulica* using wet milling with ethylene glycol, ethanol, water, or methanol using mechanochemical procedures.

The elemental composition of the raw snail shell and $CaCO_3$ nanoparticle synthesized with different solvents such as ethylene glycol, ethanol, water, and methanol is shown in Table 1. An elemental composition such as carbon, oxygen, and calcium dominated different weight percentages in both raw snail shells and the synthesized nano-$CaCO_3$. It was observed that the raw snail contains a high volume of $CaCO_3$ of about 99.4 wt.% and other metal oxides of about 6 wt.%. However, this was lesser compared to the synthesized nano-$CaCO_3$ that has 100 wt.% $CaCO_3$ irrespective of the solvent used for the wet milling process. This may suggest that the mechanochemical procedure used to synthesize helps in achieving small molecular nanoparticles and the decantation method adopted also helps in purification of the nanoparticle, resulting in clean 100 wt.% $CaCO_3$.

This performance may be a result of the milling period and solvent used. Among the nano-$CaCO_3$ synthesized with different solvents and raw snail shells, water-synthesized nano-$CaCO_3$ contains the highest amount of carbon, which eventually reduces the weight percentage of oxygen and calcium present in the material. The weight percentage of these components suggests that the use of water increases the carbon content in the synthesized $CaCO_3$, which make it harder than others; this fact can be related to the mechanical property improvement observed in Figures 2–4.

Table 2 presents particle sizes of the synthesized $CaCO_3$ nanoparticles that were investigated using iTEM Jeol 2100 HR (high resolution). To determine the appropriate solvent for optimizing the wet milling method for producing nano-$CaCO_3$, TEM images were further analyzed under TEM image analyzer software version 5.0.1 on volume base. Significantly, 28 counts of $CaCO_3$ particle sizes randomly selected were investigated against each solvent used. Figure 5 shows the TEM image analysis for $CaCO_3$ powder obtained, and the means of the powder consisted of 25.35 nm–63.68 nm sizes of a particle having semisphere morphology.

The particle size of ethanol-synthesized $CaCO_3$ ranges from 13.43 nm to 42.56 nm, ethylene glycol-synthesized $CaCO_3$ ranges from 11.56 nm to 65.78 nm, methanol-synthesized $CaCO_3$ ranges from 12.57 nm to 98.66 nm, and water-synthesized $CaCO_3$ ranges from 24.29 nm to 180.06 nm. Notably, nanosized particles within the range of 100 nm were observed for all synthesized $CaCO_3$. However, water-synthesized $CaCO_3$ has the biggest particle size of 63.68 nm, considering the mean of the 25 counts, as shown in Table 2. This particle size is consistent with figure observed in Table 1, where water-synthesized $CaCO_3$ powder has high carbon content.

The presence of water mixtures has been confirmed to affect $CaCO_3$ polymorphs and morphology [40]. This fact suggests that the inclusion of water before the milling process affected polymorphs and morphology of the shell powder, which eventually prevents the effectiveness of the ball milling process, resulting in larger particle sizes. Furthermore, ethanol-synthesized nano-$CaCO_3$ has the smallest range of particle sizes. This outcome proved the effect of ethanol on breaking $CaCO_3$ molecules into small sizes. Additionally, a low standard deviation was observed for 28 counts of $CaCO_3$ particle sizes randomly selected. This consequence depicts the effectiveness of ball milling in providing uniform particle sizes that are very close to the mean value of the particle sizes.

3.2. Mechanical Properties. The reinforcement effect of synthesized nano-$CaCO_3$ using different solvents through mechanochemical was investigated. Table 3 shows that the loading of the manufactured nanoparticle enhanced the mechanical properties of the epoxy composite. This trend is consistent with previous findings.

Table 1: Elemental composition of the raw snail shell and synthesized Nano-$CaCO_3$.

Elemental composition	Raw snail shell (wt.%)	E (wt.%)	ED (wt.%)	M (wt.%)	W (wt.%)
C	36.71	29.45	27.43	18.43	50.63
O	22.25	48.98	51.52	50.41	38.42
Ca	40.44	21.58	21.05	31.16	10.95
Calcium carbonate (wt.%)	99.4 ± 0.1	100 ± 0.1	100 ± 0.1	100 ± 0.1	100 ± 0.1
Other metal oxides	0.6 ± 0.001	—	—	—	—

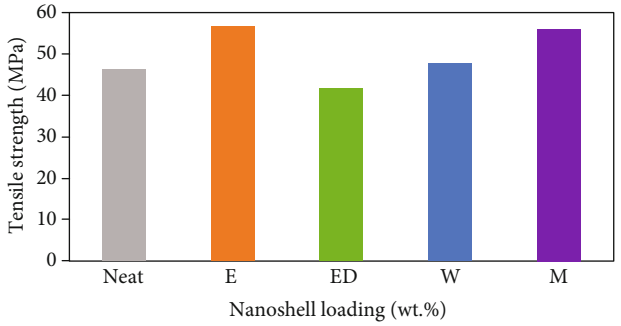

Figure 2: Tensile strength of neat and synthesized nano-$CaCO_3$-filled epoxy composites.

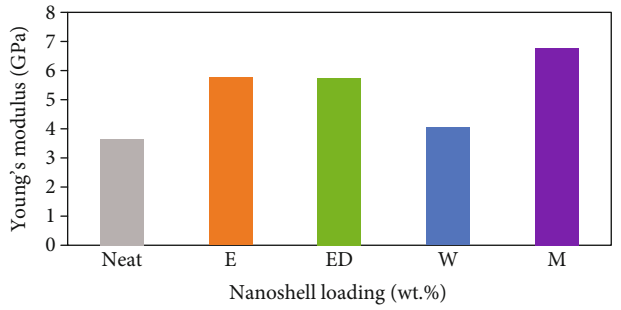

Figure 3: Tensile modulus of neat and synthesized nano-$CaCO_3$-filled epoxy composites.

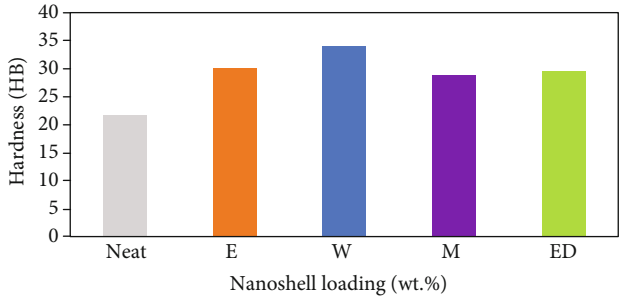

Figure 4: Hardness of neat and synthesized nano-$CaCO_3$-filled epoxy composites.

Table 2: Statistical data of the particle size of $CaCO_3$ wet milled with ethylene glycol, ethanol, water, and methanol.

Base count	E (nm)	ED (nm)	M (nm)	W (nm)
Count	28	28	28	28
Minimum	13.48	11.56	12.57	24.29
Maximum	42.90	65.78	98.66	180.06
Standard deviation	8.17	14.17	27.17	35.74
Variance	66.82	200.80	738.35	1277.52
Median	25.65	31.53	46.07	54.97
Mean	25.39	32.63	51.97	63.68

This performance may be attributed to the good dispersion and interconnecting networked structure of the particles incorporated in the matrix that formed a tougher, strengthened, and stronger structure than neat epoxy. This trend is consistent with pieces of literature where filler loading enhances mechanical properties [3, 8, 41]. The mechanical property results shown in Table 3 are higher compared with those reported in some available literature where $CaCO_3$ synthesized from other shells are used to improved mechanical properties [42–44]. The loading of $CaCO_3$ synthesized from a shell such as eggshell and mollusk and milled to microparticles improved the mechanical properties; however, loading of *Achatina fulica* shell offered superior properties [45–47]. This performance may be attributed to excellent dispersion of particles in the polymeric material shown in Figure 6, which was facilitated by the small particle sizes of the synthesized calcium carbonate particles.

Nano-$CaCO_3$ produced with ethanol- and methanol-filled composites exhibited almost the same tensile strength and hardness properties, as shown in Figures 2 and 4. The loading of nano-$CaCO_3$ synthesized with ethanol improved the strength of epoxy by 22.42%, and incorporation of nano-$CaCO_3$ manufactured by methanol enhanced tensile strength by 21.34%. This improvement may be attributed to the particle size and shape of the synthesized nano-$CaCO_3$ incorporated.

Tensile strength values for the epoxy composite filled with nano-$CaCO_3$ synthesized with ethanol glycol and water are on the lower side compared to nano-$CaCO_3$ produced with the ethanol- and methanol-filled composites. On the contrary, hardness properties for nano-$CaCO_3$ synthesized with ethanol glycol- and water-filled composites were superior to those of nano-$CaCO_3$ produced with ethanol- and methanol-filled composites as represented in Figure 4. This confirmed that the loading of nano-$CaCO_3$ synthesized with ethanol glycol and water increases hardness, which makes it brittles. The brittleness of this material is the

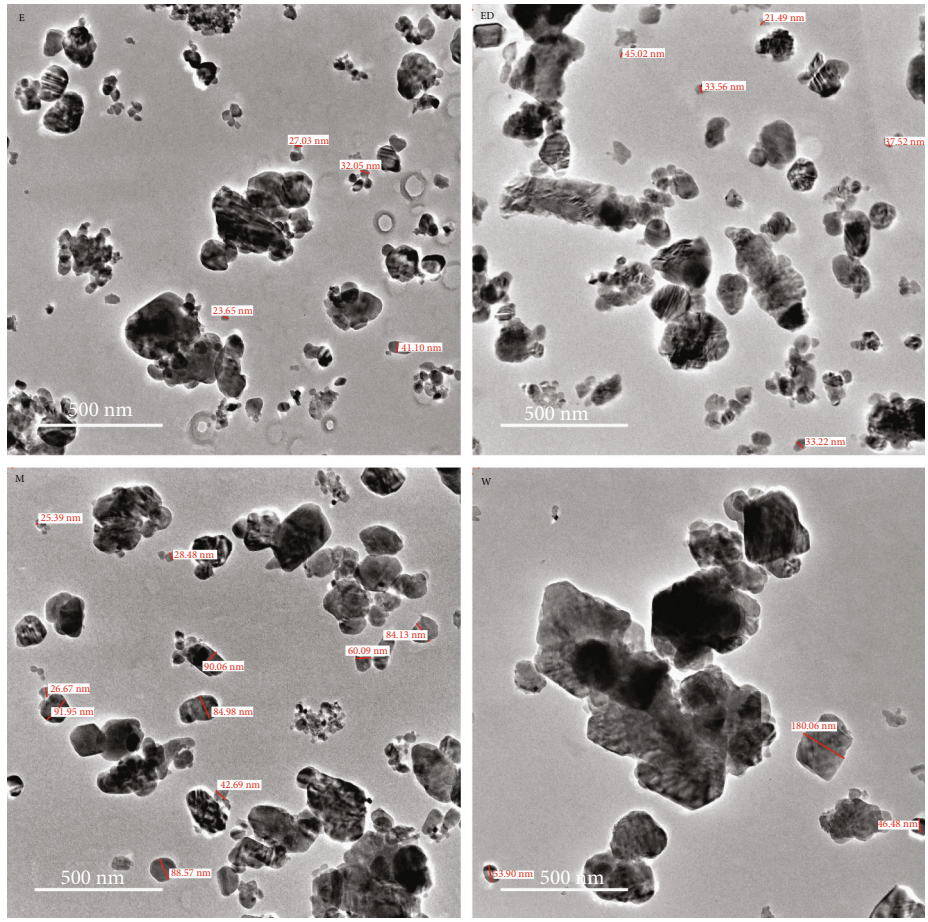

Figure 5: iTEM micrograph showing particle sizes of $CaCO_3$ obtained from ethanol (E), ethylene glycol (ED), methanol (M), water (W), and snail shell powder mixture.

Table 3: Mechanical properties of synthesized nano-$CaCO_3$-filled epoxy composite.

Samples	Tensile ultimate strength (GPa)	Young's modulus (GPa)	Hardness
Neat	46.19	3.66	21.75
E	56.55	5.77	30.15
ED	41.65	5.74	29.55
W	47.80	4.05	33.95
M	56.05	6.77	28.86

reflection of low tensile strength offered by this composite, as shown in Figure 2.

Figure 3 shows that the loading of synthesized nano-$CaCO_3$ is not only an efficient way to improve the mechanical strength of polymeric material but also enhances stiffness. The incorporation of synthesized nano-$CaCO_3$ improved the stiffness of epoxy nanocomposite irrespective of the solvent used for synthesizing the nanoparticles. The addition of nano-$CaCO_3$ synthesized with ethanol through mechanochemical techniques increased epoxy stiffness by 57.7%, and incorporation of nano-$CaCO_3$ produced with the addition of ethanol glycol enhanced the stiffness of epoxy by 56.8%. The addition of nano-$CaCO_3$ synthesized with water through mechanochemical techniques increased epoxy stiffness by 10.65%, and the loading of nano-$CaCO_3$ wet milled with methanol improved stiffness by 84.65%. Although loading of synthesized nano-$CaCO_3$ improved stiffness, the epoxy composite filled with nano-$CaCO_3$ wet milled with methanol offered superior stiffness.

TEM images presented in Figure 6 are for the epoxy polymer filled with nano-$CaCO_3$ milled using different solvents. The dark phase of the image signifies the nano-$CaCO_3$, and the lighter phase of the image signifies the polymer matrix. The TEM micrograph not only shows the well-dispersed nano-$CaCO_3$ in the matrix but also shows that the size of the nanoparticles is slightly different. This trend complements different particle sizes of synthesized nano-$CaCO_3$ shown in Table 2. Furthermore, the homogeneous dispersion of the nanoparticle shown in the TEM image formed an interlocking structure that strengthened the epoxy composite, which eventually led to the improved mechanical properties observed in Table 3.

4. Conclusion

Nano-$CaCO_3$ was successfully synthesized from *Achatina fulica* shell. The reinforcement effect of the produced

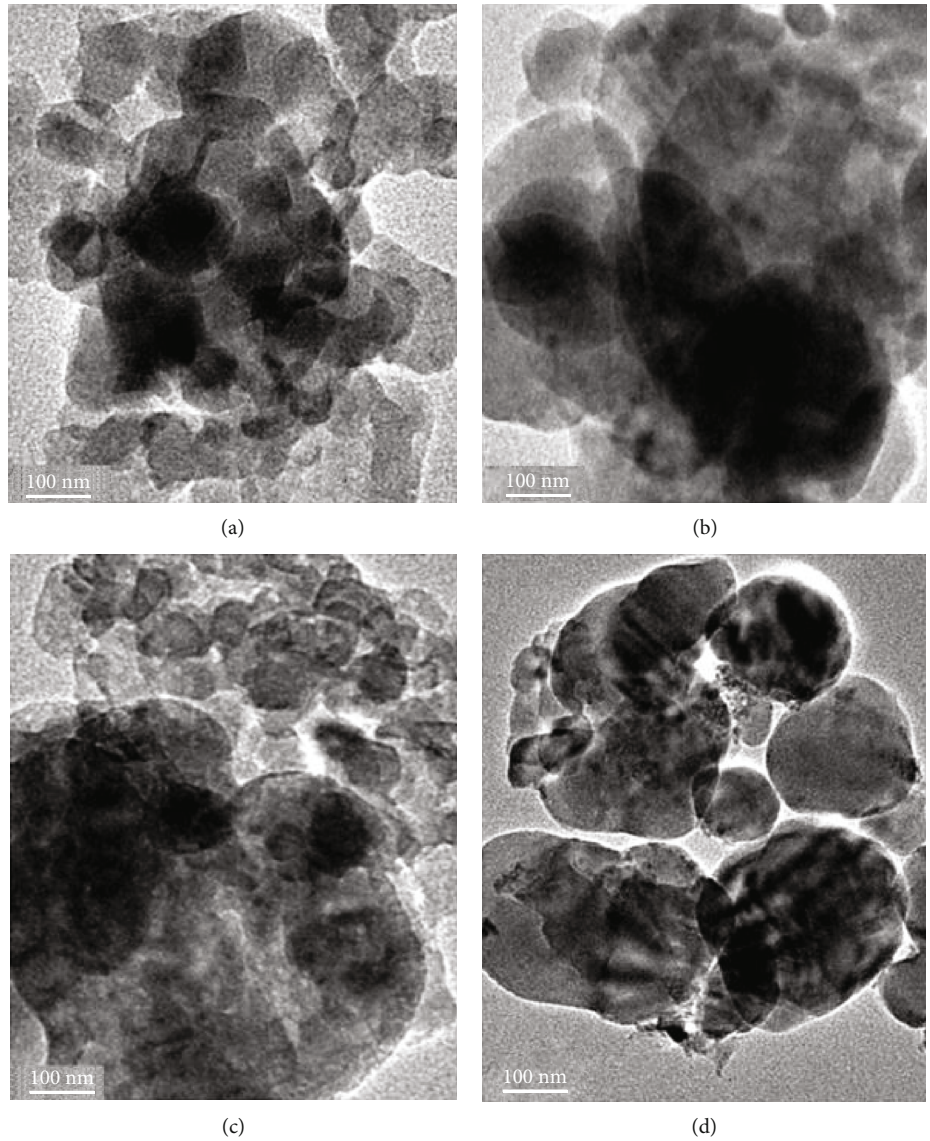

Figure 6: TEM micrograph showing the dispersion of nano-$CaCO_3$ obtained from (a) ethanol- (E-), (b) ethylene glycol- (ED-), (c) methanol- (M-), and (d) water- (W-) milled snail shell powder mixture.

nanocalcium carbonate particles, wet milled with different solvents using the mechanochemical technique, was investigated. High-speed (450 rpm) balling milling machine was used to synthesize nanoparticle sizes. The mixture of 100 mL of different solvents and 30 g of raw snail powder of particle sizes ≤ 50 nm was wet milled at 450 rpm for 258 mins in a clockwise direction to produce nano-$CaCO_3$. It was discovered that nanoparticle particle sizes (25.35 nm–63.68 nm) of calcium carbonate could be synthesized from *Achatina fulica* shell using the mechanochemical wet milling technique.

FTIR spectra for the raw shell display absorption peaks of calcite at about 713 cm^{-1} and 873 cm^{-1} and were accredited to out-of-plane bending and in-of-plane bending vibration modes, asymmetric and symmetric stretching for calcium carbonate (CO_3^{2-}) molecules. On the other hand, nano-$CaCO_3$ synthesized with different solvents such as ethylene glycol, ethanol, water, and methanol shows the absorption peaks of aragonite at around 712 cm^{-1}, 854 cm^{-1}, and 1083 cm^{-1}. The observed absorption peaks were attributed to carbonate out-of-plane bending vibrations. This bending vibration proves that milling *Achatina fulica* shell to nanoparticles changed the polymorphs of the shell powder at microsize from calcite to aragonite.

The energy-dispersive spectroscope (EDX) confirmed that the mechanochemical procedure used to synthesize nano-$CaCO_3$ from *Achatina fulica* shell helped not only in achieving small molecular nanoparticles but also in purification, resulting in unsoiled 100 wt.% $CaCO_3$. TEM image analyzer results evidenced that the $CaCO_3$ powder obtained consisted of a particle size range of 25.35 nm–63.68 nm with semisphere morphology. The mechanical property results show that the loading of nano-$CaCO_3$ synthesized from *Achatina fulica* shell through the mechanochemical procedure was an effective way of modifying mechanical strength. Although loading of synthesized nano-$CaCO_3$ improved strength and stiffness polymetric material however, the epoxy

composite filled with nano-$CaCO_3$ wet milled with methanol offered superior stiffness.

5. Future Work

The completion of this study brought forward some limitations that opened up opportunities for future work. The drawback included but not limited to the long milling period of the shells. Thus, the reduction of the milling process for synthesizing nano-$CaCO_3$ from *Achatina fulica* shell shall be a potential area for future work.

Data Availability

The authors have decided to deposit the data in the manuscript with the abovementioned topic in a public repository.

Conflicts of Interest

The authors declare that they have no conflict of interest as all authors are affiliated to the institution as academic staff and students.

Acknowledgments

The author would like to acknowledge the scholarship support towards the remission of school fees from the University of Kwazulu-Natal and financial assistance received from the CSIR and the Department of Science and Innovation (General Business Support Treasury funding).

References

[1] S. M. Dizaj, M. Barzegar-Jalali, M. H. Zarrintan, K. Adibkia, and F. Lotfipour, "Calcium carbonate nanoparticles; potential in bone and tooth disorders," *Pharmaceutical Sciences*, vol. 20, no. 4, p. 175, 2015.

[2] M. Balachandran, S. Devanathan, R. Muraleekrishnan, and S. S. Bhagawan, "Optimizing properties of nanoclay–nitrile rubber (NBR) composites using face centred central composite design," *Materials & Design*, vol. 35, pp. 854–862, 2012.

[3] M. Balachandran and S. S. Bhagawan, "Mechanical, thermal and transport properties of nitrile rubber (NBR)—nanoclay composites," *Journal of Polymer Research*, vol. 19, no. 2, p. 9809, 2012.

[4] F. Senatov, D. Kuznetsov, S. Kaloshkin, and V. Cherdyntsev, "Obtaining nanopowders of metal oxides from salts by means of mechanochemical synthesis," *Chemistry for Sustainable Development*, vol. 17, no. 6, pp. 631–636, 2009.

[5] K. Iqbal, S.-U. Khan, A. Munir, and J.-K. Kim, "Impact damage resistance of CFRP with nanoclay-filled epoxy matrix," *Composites Science and Technology*, vol. 69, no. 11-12, pp. 1949–1957, 2009.

[6] P. N. B. Reis, J. A. M. Ferreira, P. Santos, M. O. W. Richardson, and J. B. Santos, "Impact response of Kevlar composites with filled epoxy matrix," *Composite Structures*, vol. 94, no. 12, pp. 3520–3528, 2012.

[7] Y. Toledano-Magaña, L. Flores-Santos, G. M. de Oca, A. González-Montiel, J.-P. Laclette, and J.-C. Carrero, "Effect of clinoptilolite and sepiolite nanoclays on human and parasitic highly phagocytic cells," *BioMed Research International*, vol. 2015, Article ID 164980, 12 pages, 2015.

[8] T. Mohan and K. Kanny, "Thermal, mechanical and physical properties of nanoegg shell particle-filled epoxy nanocomposites," *Journal of Composite Materials*, vol. 52, no. 29, pp. 3989–4000, 2018.

[9] J. R. Woodard, A. J. Hilldore, S. K. Lan et al., "The mechanical properties and osteoconductivity of hydroxyapatite bone scaffolds with multi-scale porosity," *Biomaterials*, vol. 28, no. 1, pp. 45–54, 2007.

[10] P. Suwannasom, P. Tansupo, and C. Ruangviriyachai, "A bone-based catalyst for biodiesel production from waste cooking oil," *Energy Sources, Part A: Recovery, Utilization, and Environmental Effects*, vol. 38, no. 21, pp. 3167–3173, 2016.

[11] A. Tavangar, B. Tan, and K. Venkatakrishnan, "Synthesis of three-dimensional calcium carbonate nanofibrous structure from eggshell using femtosecond laser ablation," *Journal of Nanobiotechnology*, vol. 9, no. 1, p. 1, 2011.

[12] S. C. Onwubu, A. Vahed, S. Singh, and K. M. Kanny, "Physicochemical characterization of a dental eggshell powder abrasive material," *Journal of applied biomaterials & functional materials*, vol. 15, no. 4, 2017.

[13] M. T. Hincke, "The eggshell: structure, composition and mineralization," *Frontiers in Bioscience*, vol. 17, no. 1, article 1266, 2012.

[14] S. Patrick, V. Aigbodion, and S. Hassan, "Development of polyester/eggshell particulate composites," *Tribology in Industry*, vol. 34, no. 4, pp. 217–225, 2012.

[15] S. C. Onwubu, P. S. Mdluli, and S. Singh, "Evaluating the buffering and acid-resistant properties of eggshell–titanium dioxide composite against erosive acids," *Journal of Applied Biomaterials & Functional Materials*, vol. 17, no. 1, article 2280800018809914, 2019.

[16] S. C. Onwubu, S. Mhlungu, and P. S. Mdluli, "*In vitro* evaluation of nanohydroxyapatite synthesized from eggshell waste in occluding dentin tubules," *Journal of Applied Biomaterials & Functional Materials*, vol. 17, no. 2, article 2280800019851764, 2019.

[17] L. M. Reynard, G. M. Henderson, and R. E. M. Hedges, "Calcium isotopes in archaeological bones and their relationship to dairy consumption," *Journal of Archaeological Science*, vol. 38, no. 3, pp. 657–664, 2011.

[18] M. Baláž, "Ball milling of eggshell waste as a green and sustainable approach: a review," *Advances in Colloid and Interface Science*, vol. 256, pp. 256–275, 2018.

[19] T. Filetin, I. Žmak, S. Šolić, and S. Jakovljević, "Microhardness of mollusc seashell structures," in *Proceedings of International Conference on Innovative Technologies IN-TECH*, pp. 95–97, Prague, 2010.

[20] O. J. Gbadeyan, G. Bright, B. Sithole, and S. Adali, "Physical and morphological properties of snail (*Achatina fulica*) shells for beneficiation into biocomposite materials," *Journal of Bio- and Tribo-Corrosion*, vol. 6, no. 2, 2020.

[21] T. K. Achar, A. Bose, and P. Mal, "Mechanochemical synthesis of small organic molecules," *Beilstein Journal of Organic Chemistry*, vol. 13, no. 1, pp. 1907–1931, 2017.

[22] H. Kulla, M. Wilke, F. Fischer, M. Röllig, C. Maierhofer, and F. Emmerling, "Warming up for mechanosynthesis–temperature development in ball mills during synthesis," *Chemical Communications*, vol. 53, no. 10, pp. 1664–1667, 2017.

[23] P. Chauhan and S. S. Chimni, "Mechanochemistry assisted asymmetric organocatalysis: a sustainable approach," *Beilstein Journal of Organic Chemistry*, vol. 8, no. 1, pp. 2132–2141, 2012.

[24] R. Stevenson and G. De Bo, "Controlling reactivity by geometry in retro-diels–alder reactions under tension," *Journal of the American Chemical Society*, vol. 139, no. 46, pp. 16768–16771, 2017.

[25] J. L. Howard, W. Nicholson, Y. Sagatov, and D. L. Browne, "One-pot multistep mechanochemical synthesis of fluorinated pyrazolones," *Beilstein Journal of Organic Chemistry*, vol. 13, no. 1, pp. 1950–1956, 2017.

[26] A. D. McNaught and A. D. McNaught, *Compendium of Chemical Terminology*, Blackwell Science Oxford, 1997.

[27] P. Baláž, *Mechanochemistry in Nanoscience and Minerals Engineering, Mechanochemistry in Nanoscience and Minerals Engineering*, Springer, Berlin, Heidelberg, 2008.

[28] H. X. Kho, S. Bae, S. Bae, B.-W. Kim, and J. S. Kim, "Planetary ball mill process in aspect of milling energy," *Journal of Korean powder metallurgy institute*, vol. 21, no. 2, pp. 155–164, 2014.

[29] M. Broseghini, L. Gelisio, M. D'Incau, C. L. Azanza Ricardo, N. M. Pugno, and P. Scardi, "Modeling of the planetary ball-milling process: the case study of ceramic powders," *Journal of the European Ceramic Society*, vol. 36, no. 9, pp. 2205–2212, 2016.

[30] D. Das, Z. T. Bhutia, A. Chatterjee, and M. Banerjee, "Mechanochemical Pd (II)-catalyzed direct and C-2-selective arylation of indoles," *The Journal of Organic Chemistry*, vol. 84, no. 17, pp. 10764–10774, 2019.

[31] D. Margetic and V. Štrukil, *Mechanochemical Organic Synthesis*, Elsevier, 2016.

[32] J. Franke and A. Mersmann, "The influence of the operational conditions on the precipitation process," *Chemical Engineering Science*, vol. 50, no. 11, pp. 1737–1753, 1995.

[33] M. Vučak, J. Perić, and R. Krstulović, "Precipitation of calcium carbonate in a calcium nitrate and monoethanolamine solution," *Powder Technology*, vol. 91, no. 1, pp. 69–74, 1997.

[34] G. O. Falope, A. G. Jones, and R. Zauner, "On modelling continuous agglomerative crystal precipitation via Monte Carlo simulation," *Chemical Engineering Science*, vol. 56, no. 7, pp. 2567–2574, 2001.

[35] M.-H. Sung, I.-S. Choi, J.-S. Kim, and W.-S. Kim, "Agglomeration of yttrium oxalate particles produced by reaction precipitation in semi-batch reactor," *Chemical Engineering Science*, vol. 55, no. 12, pp. 2173–2184, 2000.

[36] S. C. Onwubu, P. S. Mdluli, S. Singh, S. Nyembe, and R. Thakur, "Corrigendum to "An in situ evaluation of the protective effect of nano eggshell/titanium dioxide against erosive acids"," *International Journal of Dentistry*, vol. 2019, Article ID 7209168, 1 pages, 2019.

[37] D. Chakrabarty and S. Mahapatra, "Aragonite crystals with unconventional morphologies," *Journal of Materials Chemistry*, vol. 9, no. 11, pp. 2953–2957, 1999.

[38] F. Reig, "FTIR quantitative analysis of calcium carbonate (calcite) and silica (quartz) mixtures using the constant ratio method. Application to geological samples," *Talanta*, vol. 58, no. 4, pp. 811–821, 2002.

[39] I. M. Weiss, N. Tuross, L. Addadi, and S. Weiner, "Mollusc larval shell formation: amorphous calcium carbonate is a precursor phase for aragonite," *Journal of Experimental Zoology*, vol. 293, no. 5, pp. 478–491, 2002.

[40] K. K. Sand, J. D. Rodriguez-Blanco, E. Makovicky, L. G. Benning, and S. L. S. Stipp, "Crystallization of $CaCO_3$ in water–alcohol mixtures: spherulitic growth, polymorph stabilization, and morphology change," *Crystal Growth & Design*, vol. 12, no. 2, pp. 842–853, 2012.

[41] O. J. Gbadeyan, K. Kanny, and M. T. Pandurangan, "Tribological, mechanical, and microstructural of multiwalled carbon nanotubes/short carbon fiber epoxy composites," *Journal of Tribology*, vol. 140, no. 2, 2018.

[42] S. O. Adeosun, E. I. Akpan, and H. A. Akanegbu, "Thermomechanical properties of unsaturated polyester reinforced with coconut and snail shells," *International Journal of Composite Materials*, vol. 5, no. 3, pp. 52–64, 2015.

[43] P. U. Chris-Okafor, C. C. Okonkwo, and M. S. Ohaeke, "Reinforcement of high density polyethylene with snail shell powder," *American Journal of Polymer Science*, vol. 8, no. 1, pp. 17–21, 2018.

[44] G. C. Onuegbu and I. O. Igwe, "The effects of filler contents and particle sizes on the mechanical and end-use properties of snail shell powder filled polypropylene," *Materials Sciences and Applications*, vol. 2, no. 7, pp. 810–816, 2011.

[45] C. Onuoha, O. Onyemaobi, C. Anyakwo, and G. Onuegbu, "Effect of filler loading and particle size on the mechanical properties of periwinkle shell filled recycled polypropylene composites," *American Journal of Engineering Research*, vol. 6, no. 4, pp. 72–79, 2017.

[46] O. J. Gbadeyan, S. Adali, G. Bright, B. Sithole, and O. Awogbemi, "Studies on the mechanical and absorption properties of achatina fulica snail and eggshells reinforced composite materials," *Composite Structures*, vol. 239, p. 112043, 2020.

[47] R. Umunakwe, O. Okoye, U. Nwigwe, A. Oyetunji, and I. Umunakwe, "Effects of stirring time and particles preheating on porosity, mechanical properties and microstructure of periwinkle shell-aluminium metal matrix composite (PPS-ALMMC)," *Annals of the Faculty of Engineering Hunedoara*, vol. 15, no. 3, p. 133, 2017.